NASA Technical Memorandum 106506

Matrix Fatigue Cracking Mechanisms of α_2 TMC for Hypersonic Applications

Timothy P. Gabb and John Gayda
Lewis Research Center
Cleveland, Ohio

Prepared for
Life Prediction Methodology for Titanium Matrix Composites
sponsored by the American Society for Testing and Materials
Hilton Head, South Carolina, March 22-24, 1994

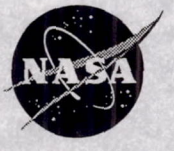

National Aeronautics and
Space Administration

Matrix Fatigue Cracking Mechanisms of α_2 TMC for Hypersonic Applications

Timothy P. Gabb and John Gayda
National Aeronautics and Space Administration
Lewis Research Center
Cleveland, Ohio 44135

ABSTRACT: The objective of this work was to understand matrix cracking mechanisms in a unidirectional α_2 TMC in possible hypersonic applications. A $[0]_8$ SCS-6/Ti-24Al-11Nb(at.%) TMC was first subjected to a variety of simple isothermal and nonisothermal fatigue cycles to evaluate the damage mechanisms in simple conditions. A modified ascent mission cycle test was then performed to evaluate the combined effects of loading modes. This cycle mixes mechanical cycling at 150 and 483°C, sustained loads, and a slow thermal cycle to 815°C. At low cyclic stresses and strains more common in hypersonic applications, environment-assisted surface cracking limited fatigue resistance. This damage mechanism was most acute for out-of-phase nonisothermal cycles having extended cycle periods and the ascent mission cycle. A simple linear fraction damage model was employed to help understand this damage mechanism. Time-dependent environmental damage was found to strongly influence out-of-phase and mission life, with mechanical cycling damage due to the combination of external loading and CTE mismatch stresses playing a smaller role. The mechanical cycling and sustained loads in the mission cycle also had a smaller role.

Introduction

Titanium alloy matrix composites (TMCs) have potential in aerospace structural applications requiring high strength and stiffness combined with low density. In gas turbine engines, these composites are being considered for highly stressed rotating components such as compressor disks and blades, and a variety of static components [1]. In projected hypersonic applications, composites have been considered for airframe panels consisting of skins with stiffeners and joints [2].

Investigations of the fatigue response of TMCs have provided some insights of TMC fatigue failure mechanisms possible in such applications. Fatigue loading of unidirectional 0° fiber reinforced composites foreseen in rotating components at high cyclic stresses such as disks can induce stress relaxation in the matrix, where some of the load is shifted to the fibers. In load controlled fatigue conditions this can cause fiber dominated failures [3,4]. This failure mode is accentuated in cycles where maximum loads are concentrated at maximum temperatures, such as isothermal fatigue tests with maximum load dwells [5], and in-phase thermomechanical fatigue tests [6,7]. However, in fatigue loading of unidirectional 0° fiber reinforced composites at the lower cyclic stresses foreseen in hypersonic applications, the fatigue durability is often limited by matrix cracking mechanisms [3-7] for isothermal fatigue and thermomechanical fatigue. Composites of other laminate orientations such $[90]_8$, $[0/90]_s$, and $[0/\pm45/90]_s$ having off axis fibers also suffer fiber-matrix debonding in isothermal [9,10] and thermomechanical [11,12,13] fatigue, and matrix cracks often

initiate at the debonded interfaces. Comparative tests in vacuum [14,15] indicate the environment has a role in many of these matrix cracking mechanisms. α_2 titanium alloys generally have better high temperature strength and environmental resistance than ß titanium alloys [16] and could therefore have potential applications in hypersonic cycles where temperatures approach 815°C.

The objective of this study was to investigate these matrix cracking mechanisms in a unidirectional 0° fiber reinforced α_2 TMC at low applied stresses to determine the primary factors driving these mechanisms in TMCs and the governing factor/damage relationships. Isothermal fatigue and nonisothermal fatigue tests were first employed to understand the failure mechanisms induced in simple fatigue cycles which were relevent to hypersonic load-temperature-time service cycles. A more complex modified hypersonic ascent mission cycle was then employed to evaluate the damage modes in more realistic conditions where several loading modes are superimposed at variable temperatures. A linear life fraction damage model was applied to aid in understanding the relative contributions of the different loading and damage modes.

Experimental Procedure

The composite test material was made of Ti-24Al-11Nb (at. %) matrix, reinforced by 35 v/o of SCS-6 SiC fibers oriented at 0° to the specimen loading axis, Fig. 1. This composite was fabricated by Textron Specialty Materials through foil-fiber processing. The fibers were first woven with Ti-Nb wire crossweave into unidirectional mats. Eight alternating layers of matrix foil and 0°

fiber mat were then arranged and consolidated by hot isostatic pressing to form $[0]_8$ panels. Rectangular and reduced midsection specimens each having gage sections 12.5 mm long, 6.3 mm wide, and 1.6 mm thick were waterjet machined from the panels. Load controlled fatigue tests were performed in air on a servohydraulic test system utilizing direct induction heating and an axial extensometer. As shown in the load and temperature waveforms of Fig. 2, standard fatigue (SF) tests were first performed at 0.33 Hz and R_σ=0 (minimum/maximum stress ratio) at constant temperature. Simple nonisothermal tests where load and temperature are sequentially cycled were then performed to simplify initial damage analyses. Load was applied at minimum temperature for the out-of-phase (OP) tests and at maximum temperature for several comparative in-phase (IP) tests. More complex nonisothermal and hypersonic mission cycles were subsequently performed, as will be described later. Failure for all cyclic types is defined as complete specimen fracture into two pieces. The damage mechanisms induced in interrupted and failed test specimens were subsequently characterized with optical and scanning electron microscopy.

Results and Discussion

1. Isothermal and Nonisothermal Fatigue

In all test types, cyclic life increased with decreasing stress range as usual [5]. Fig. 3 compares cyclic life at an equivalent stress range of about 690 MPa and mechanical strain range of about 0.40%. Standard isothermal fatigue life decreased with increasing temperature, however OP cycling was life-limiting

at these low stress ranges. The operative damage mechanisms are evident from the fracture surfaces shown in Fig. 4. Standard isothermal fatigue at 150°C induced relatively few surface-initiated fatigue cracks that propagated long distances. Standard isothermal fatigue at 650°C induced relatively few fatigue cracks initiating principally at damaged fibers on the specimen edges. These cracks grew moderate distances. IP cycling from 150 to 650°C induced edge cracking similar to 650°C standard fatigue. OP cycling from 150 to 650°C induced a different damage mechanism of enhanced surface crack initiation in the matrix. The growth of the out-of-phase cracks subsequently allowed considerable fiber-matrix interface oxidation and damage. Examination of metallographic sections of the test specimens indicated that in each of these cases, cracks preferentially grew in the matrix while the fibers often remained uncracked near the crack tip [5].

The factors driving these matrix cracking mechanisms were then explored by performing a series of isothermal and nonisothermal tests varying temperature cycle range (ΔT) and maximum temperature (T_{max}) at a constant stress range. OP rather than IP nonisothermal cycling was selected for this evaluation, due to the lower life and increased matrix cracking of the OP cycle at low cyclic stresses. Resulting fatigue life is shown as a function of ΔT in Fig. 5a. Isothermal fatigue life decreased consistently when going form 150 to 815°C. But OP life was always much lower than the isothermal life at the same loading temperature. As clearly shown for a loading temperature of 150°C, fatigue life consistently decreased with increasing ΔT for a given loading temperature. However life

varied with loading temperature. Life is expressed as a function of T_{max} in Fig. 5b. OP life was more closely related to T_{max}. OP damage correspondingly increased with increasing T_{max}, as shown by comparing the specimen surfaces in Fig. 6. Standard isothermal fatigue also produced considerable surface cracking at 815°C, as shown in Figure 6. This suggested time and temperature-dependent environmental effects were dominating damage and life in both isothermal and nonisothermal tests at high temperatures, and that a single damage relationship might be able to describe the damage processes.

2. Linear Damage Formulation

Damage relationships were quantitatively evaluated to aid understanding, using an approach similar to that of Nicholas and Russ [17]. The purpose of this modelling was only to provide some understanding of the factor/damage relationships, rather tnan to provide a generalized TMC life prediction model. A simple linear summation of mechanical damage $\Sigma\ N/N_m$ and time-dependent environmental damage $\Sigma\ N\ P/t_E$ was applied, where N is the number of cycles, N_m is the mechanical life at a strain range $\Delta\epsilon_m$ and temperature T, and t_E is the accumulated time to failure at cycle period P and temperature T. For isothermal and nonisothermal OP cyclic life this simplifies [18] to:

$$1/N_m + \Sigma\ P/t_E = 1/N_f\ ,$$

where the time-temperature waveform of the OP cycle is approximated with isothermal segments of 1 second duration to determine $\Sigma\ P/t_E$.

Environmental damage relationships were characterized with isothermal fatigue cycles with σ_{max}=690 MPa and dwells at zero load to vary cycle period. This would incorporate fatigue influences, however such an approach precluded application to monotonic creep tests which were not a subject of this investigation. Fig. 7 depicts the accumulated time to failure versus cycle period in tests at several temperatures. Accumulated time to failure t_E did not vary appreciably with cycle period over this range. This suggested an environmental damage relationship based on simple summation of time at a temperature could be applicable under these test conditions. The accumulated time to failure decreased with increasing temperature, reflecting the increasing damage severity with increasing T_{max}. This gave the environmental damage term Σ P/t_E as a function of temperature. Mechanical damage relationships were characterized with isothermal fatigue tests run at σ_{max}=690 MPa in argon at a high frequency of 5 Hz to minimize time-dependent environment effects. In comparison to air tests, cyclic life increased in the 5 Hz, argon tests. However these tests failed at lower accumulated times than tests in air. Therefore, it was assumed that mechanical damage was dominant, and that environmental damage was minimized. These tests gave mechanical fatigue life and the mechanical damage term, $1/N_m$, as a function of temperature, Fig. 8.

OP cycling produces higher mechanical cyclic strains in the matrix than isothermal tests, due to thermal expansion mismatch strains generated by the ΔT. The mechanical damage in OP tests was therefore adjusted for the additional thermal mismatch strains

generated in the matrix along the axial direction, normal to observed surface cracking. The axial thermal mismatch strain was approximated as $(\alpha_{matrix}-\alpha_{comp.})\Delta T$ and added to the applied mechanical strain for OP cycling to give the total matrix strain. A strain range - fatigue life line was not available from the argon environment tests. The mechanical damage life at the loading temperature was instead multiplied by the ratio of lives observed in tests at the applied and total matrix strain ranges performed at 150°C in air. This provided some measure of the magnitude of the out-of-phase cycles' CTE effects on mechanical damage. The damage relationships generated from isothermal tests could now be utilized to handle both isothermal and nonisothermal OP life.

The simple damage formulation predicted nonisothermal OP life fairly well using the isothermally generated relationships. Calculated fatigue lives are compared to observed fatigue lives for standard fatigue, isothermal dwell, and OP tests in Fig. 9. Calculated isothermal lives agree well with observed lives, indicating the model properly reproduces the data employed in deriving the relationships. OP life is predicted within about 2X of observed life. The environmental damage term contributed most of the damage in tests at high T_{max} and low life, while the mechanical damage term began to contribute substantial damage in low T_{max}, long life tests. This is consistent with the propensity of surface cracking observed experimentally. OP life predictions at high T_{max} and low life were consistently higher than experimental data. This may indicate the presence of additional environmental damage attributable to TMF-environment interactions, not included in the

simple damage formulation. But the simple damage formulation still profided a useful tool for comparing mechanical and environmental sources of damage in different cycles. Additional linear fraction damage interaction terms have been successfully developed by Neu and Nicholas [19].

3. Hypersonic Service Cycles

Actual hypersonic structural applications will produce complex service cycles mixing cyclic loads, sustained loads, and multiple temperature changes. It is important to understand the effects of such cycles on durability and failure mechanisms. Additional tests were therefore performed to evaluate these effects. An ascent mission cycle [20] was chosen and modified to represent an example service cycle, shown in Fig. 10. This cycle has subcycling at 150 and 425°C, intermediate sustained loads, and a slow thermal ramp from 425 to 815°C. The maximum applied stress was again 690 MPa, but the cycle period was 26 minutes. This mission cycle does have OP cycle traits, with maximum applied stresses attained at low-intermediate temperatures within the cycle. The average mission cycle life of duplicate tests was only 101 cycles. SEM micrographs of mission cycle fracture surfaces and gage sections indicated the dominant damage mechanism was again environment-assisted surface cracking.

The mission cycle life of 101 cycles was much lower than the OP life of 764 cycles at the same maximum stress of 690 MPa and ΔT of 150-815°C. Several characteristics unique to the mission cycle could explain the lower life of the mission cycle. Sustained loads

were present throughout the cycle. Subcycling was applied at low and intermediate temperatures. The cycle time was much longer than the standard OP cycle period. A series of tests were performed to understand the effects of each of these service characteristics. These tests were all performed with a maximum temperature of 815°C, and a maximum stress of 690 MPa.

Several tests were performed to evaluate the effects of sustained load. A creep test was performed at maximum stress and maximum temperature. A specimen was thermally cycled from 150 to 815°C at a sustained stress of 690 MPa. The resulting lives are compared to standard OP and mission cycle lives in Fig. 11. The creep test was interrupted at 526 hours with no signs of matrix surface cracking. The thermal cycling life was comparable to the standard OP life on both a time to failure and cycles to failure basis, and had comparable surface cracking damage. However, the thermal cycling life did not approach the low mission cycle life. The simple damage formulation was not specifically designed to handle sustained loads. However, a thermal cycling life prediction using the model's environmental damage term P/t_E alone was within 2X, Fig. 11. These sustained load tests indicated even severe sustained loads were no more damaging than a cyclic load applied at minimum temperature.

Subcycling effects were evaluated in tests using the standard OP thermal cycle, with a block of n subcycles applied at 1 Hz at the minimum temperature of 150°C between each thermal cycle at zero load to 815°C. The resulting lives in blocks to failure are shown as a function of subcycles per block in Fig. 12. Subcycling did not

strongly influence OP life and could not explain the reduced mission cycle life. The additional mechanical damage produced by even 200 subcycles between each thermal cycle was predicted to remain small relative to the environmental damage and have little effect on OP life, consistent with the experimentally observed trend.

The preceding tests have shown severe sustained applied stresses were no more damaging than the same cyclic stress applied at minimum temperatures, and did not strongly influence OP life. Subcycling did not strongly influence OP life. These results suggested the low mission cycle life was largely due to the additional environmental effects incurred by the extended mission cycle period. This indicated a simple standard OP cycle with an extended cycle period might largely reproduce the mission cycle damage and life.

An OP test was performed with an extended cycle period of 26 minutes. Life as a function of cycle period is compared for OP and mission cycles tests in Fig. 13. An extended cycle period reduced OP life to the mission cycle levels. Comparison of the specimen gage surfaces in Fig. 14 show severe environment assisted surface cracking in both extended cycle period and mission tests. The slow nonisothermal OP test appears to be a useful simple screening test for resistance to environment assisted surface cracking in hypersonic applications, as both the slow OP and mission test lives are dominated by this time-dependent environment driven damage. The linear fraction model was applied to the slow OP cycle as before. Based on the results of previous tests of mission cycle effects, an

attempt could be made to also employ the model to predict mission cycle life. Sustained loads were handled as previously described. Subcycling mechanical damage was computed as before, with a simple stress ratio correction using a simplified Goodman approach. Both predictions were within 2X, with time dependent environmental damage term strongly dominating in both cases. The additional mechanical damage contributed by the mission's subcycling was negligibly small, so that the slow OP and mission cycle life predictions were essentially the same.

Observed fatigue lives are compared to lives calculated using the simple linear fraction damage formulation for all tests in Fig. 15. This simple formulation did a reasonable job predicting the nonisothermal lives, which span several orders of magnitude. This appears to be due in part to the very strong effects of time-dependent environment driven damage in elevated temperature tests, including the ascent mission cycle.

4. Out-of-Phase Environment Assisted Surface Cracking

The results indicate that a most serious, life-limiting cracking mechanism in hypersonic applications could be associated with OP environment assisted cracking. Environment assisted surface cracking was enhanced in these OP tests over that in isothermal and isothermal dwell tests having comparable times at high temperatures. Further, a creep test at 815°C and 690 MPa did not produce significant surface cracking after 526 hours. This indicated environment assisted surface cracking was not proportional to only time at high temperatures. These facts

suggested the low OP and mission lives were due to surface cracking enhanced by TMF-environment interactions. In order to experimentally explore this, the damage of the thermal and loading cycles of the OP test were evaluated separately. A specimen was first subjected to 750 thermal cycles from 150 to 815°C at zero load and then examined. Although the surface was oxidized, only a very few minor surface cracks up to 0.4 mm long were observed, Fig. 17a. This specimen was then fatigue tested at 150°C and 690 MPa. This test was interrupted after 738,930 cycles and produced relatively few large surface cracks as in standard 150°C isothermal fatigue tests, Fig. 17b. A thermal cycle to high temperatures immediately followed by or combined with an applied tensile load at low temperatures apparently interact to produce much more environment assisted surface cracking damage than that produced separately by thermal cycling followed by low temperature fatigue cycling. It should be noted that the simple linear damage formulation would predict the same damage and life in this damage separation test as in the conventional OP test, as it has no cycle or damage sequence dependencies. This illustrates that such a simple formulation artificially separates the damage of an inherently combined damage mechanism. While such a formulation is a useful tool, it does not completely describe or predict such complex damage mechanisms.

An oxygen-affected surface layer forms in the titanium aluminide matrix during high temperature excursions. This region has been shown [21] to be made up of a non-protective brittle oxide rich in TiO_2 over matrix embrittled by additional oxygen in solid

solution. An applied cyclic load could preferentially crack this brittle region. As the kinetics of titanium oxide formation and oxygen diffusion in titanium are rapid, the embrittling effect of oxygen could advance beyond a crack tip during each thermal cycle. The crack could then advance through this embrittled region in subsequent loading, especially during low temperature loading where the ductility of titanium alloys such Ti-24Al-11Nb generally decreases with decreasing temperature.

The environment assisted surface cracking mechanism may be difficult to prevent in titanium matrix composites. Titanium alloys (greater than 50 atomic % titanium) generally form TiO_2 rich oxide layers at temperatures approaching 815°C, and have high oxygen diffusivities. γ TiAl alloys have a more protective Al_2O_3 oxide at temperatures up to 815°C and could offer improved resistance to this cracking. TMC coatings or claddings of more oxidation resistant materials may offer benefits, provided crack initiation problems of even ductile coatings can be surmounted [20]. The effects of environment assisted surface cracking could be reduced at the low partial pressures of oxygen foreseen during high elevation, high temperature segments of the hypersonic service cycles. Out-of-phase testing of SCS-6/Ti-24-11 in flowing argon containing 10^{-6} ppm of oxygen increased life by more than 100X over tests in air [15]. However, surface crack initiations in the matrix still limited life even at this low oxygen level, and therefore still could do so in many hypersonic applications.

Summary and Conclusions

TMC fatigue damage mechanisms involving matrix cracking were evaluated at low applied stresses in $[0]_8$ SCS-6/Ti-24Al-11Nb TMC. Simple isothermal and nonisothermal fatigue tests were first performed to understand the basic factor damage relationships. More complex cycles mixing cyclic loads, sustained loads, and multiple temperature changes were then employed to extend this understanding to complex service cycles. Matrix cracking occurred in both isothermal and nonisothermal tests. Time dependent environment assisted surface cracking was activated in tests to high temperatures. This environment assisted surface cracking was enhanced to produce lowest lives in out-of-phase fatigue tests having extended cycle periods. It can be concluded from this work that:

1) Matrix cracking mechanisms can often limit the fatigue durability of unidirectional 0° fiber TMC such as SCS-6/Ti-24Al-11Nb.
2) Environment assisted surface cracking in the matrix can occur in out-of-phase service cycles which combine low temperature tensile loads with high temperature excursions to most seriously limit TMC durability. The slow out-of-phase characteristics of the hypersonic ascent mission cycle largely governed life.
3) The governing factor-damage relationships could be modelled reasonably well with a linear damage formulation for these test conditions, however the enhanced out-of-phase cracking mechanism has an inherent out-of-phase TMF-environment

interaction which is not fully described in this formulation.

4) This enhanced environment assisted matrix surface cracking may have reduced effects in hypersonic applications with high temperature exposures at low oxygen partial pressures, but the cracking may well still occur and limit life.

Acknowledgements

The authors wish to gratefully acknowledge the support of the National Institute for the Mechanics & Life Prediction of High Temperature Composites.

Table 1--Tabulated Fatigue Test Results.

TEST TYPE	STRESS (MPa)	PERIOD (sec.)	STRAIN RANGE(%)/MAX STRAIN(%) CYCLE 1	CYCLE 100	HALF LIFE	LIFE (cycles)
150C SF	723	1	.45/.45	.40/.48	.49/.68	726,790+
483C SF	690	3	.40/.40	.38/.42	.38/.45	292,842
650C SF	682	3	.43/.43	.40/.45	.40/.49	40,225
650C SF	690	3	.41/.41	.40/.44	.42/.49	52,056
650C SF	685	3	.38/.38	.38/.40	.40/.46	100,950
815C SF	689	3	.45/.45	.43/.48	.44/.52	15,171
815C SF	632	3	.41/.41	.38/.44	.40/.48	16,750
483C DWELL	715	64	.38/.38	.39/.38	.40/.38	20,642
650C DWELL	690	10	.37/.37	.38/.39	.38/.40	12,878
650C DWELL	689	63	.42/.42	.42/.44	.43/.45	4,543
815C DWELL	695	64	.44/.44	.44/.45	.45/.46	748
150-483C OP	695	80	.42/.42	.41/.47	.51/.67	39,629
150-483C OP	696	63	.39/.39	.36/.39	.40/.53	42,776
150-650C OP	688	120	.40/.40	.37/.41	.46/.57	5,260
150-650C OP	753	111	.48/.48	.43/.48	.51/.55	4,861
150-815C OP	687	129	.43/.43	.37/.43	.42/.52	751
150-815C OP	723	131	.44/.44	.40/.44	.45/.52	777
483-815C OP	684	86	.41/.41	.38/.42	.40/.45	816
483-815C OP	701	70	.41/.41	.38/.41	.38/.42	985
650-815C OP	694	43	.39/.39	.38/.40	.38/.40	1,482
MISSION CYC	690	1710	-/.51	-/-	-/.51	94
MISSION CYC	684	1710	-/.53	-/.66	-/.57	108
815C CREEP	690		-/.49	-/-	-/.58	526 HR+
150-815C TC	689	130	-/.45	-/.47	-/.48	1122
OPSUB 20	694	252	.40/.40	.38/.41	.44/.52	866
OPSUB 200	692	386	.40/.40	.35/.38	.44/.51	773
OPSUB 5000	697	5436	.38/.38	.45/.54	-/-	158+
150-815C OP	688	1560	.38/.38	.39/.45	.38/.44	161
150C TC+SF	688	130+1	.37/.37	.34/.38	.37/.41	738,930+

SF - STANDARD ISOTHERMAL FATIGUE
OP - OUT-OF-PHASE
DWELL - ISOTHERMAL FATIGUE WITH DWELL AT ZERO LOAD
OPSUB XX - OUT-OF-PHASE WITH XX LOAD CYCLES/150-815C THERMAL CYCLE
TC - THERMAL CYCLES WITH STATIC LOAD
TC+SF - 750 THERMAL CYCLES AT 150-815C & ZERO LOAD THEN 150C SF

References

[1] Larsen, J. M., Russ, S. M., and Jones, J. W., "Possibilities and Pitfalls in Aerospace Applications of Titanium Matrix Composites," Proc. of the AGARD Conf. on the Characterization of Fiber Reinforced Titanium Metal Matrix Composites, Bordeaux, France, Sept. 1993.

[2] Sorensen, J., "Titanium Matrix Composites - NASP Materials and Structures Augmentation Program," AIAA Report AIAA-90-5207, American Institute of Aeronautics and Astronautics, Washington, D.C., 1990.

[3] Gayda, J., Gabb, T. P., and Freed, A. D., "The Isothermal Fatigue Behavior of a Unidirectional SiC/Ti Composite and the Ti Alloy Matrix," in Fundamental Relationships Between Microstructure and Mechanical Properties of Metal Matrix Composites, P. K. Liaw and M. N. Gungor, Ed., TMS-AIME, Warrendale, PA, 1990, pp. 497-514.

[4] Majumdar, B. S. and Newaz, G. M., "Isothermal Fatigue Failure Mechanisms in Ti-Based Metal Matrix Composites," NASA Contract Report CR-191181, National Aeronautics and Space Administration, Lewis Research Center, Cleveland, OH, 1993.

[5] Gabb, T. P. and Gayda, J., "Isothermal and Nonisothermal Fatigue Damage/Failure Mechanisms in SiC/Ti-14Al-21Nb," Titanium Matrix Composites, Workshop Proceedings, WL-TR-92-4035, P. R. Smith and W. C. Revelos, Eds., Wright Laboratory, Wright-Patterson Air Force Base, OH, 1992, pp. 292-305.

[6] Castelli, M. G., Bartolotta, P. A., and Ellis, J. R., "Thermomechanical Testing of High-Temperature Composites:

Thermomechanical Fatigue (TMF) Behavior of SiC(SCS-6)/Ti-15-3" Composite Materials: Testing and Design, ASTM STP 1120, G. C. Grimes, Ed., American Society for Testing and Materials, Philadelphia, PA, 1992, pp. 70-86.

[7] Russ, S. M., Nicholas, T., Bates, M., and Mall, S., "Thermomechanical Fatigue of SCS-6/Ti-24Al-11Nb Metal Matrix Composite," Proc. of Symp. on Failure Mechanisms in High Temperature Composites, American Society for Mechanical Engineers, 1991.

[8] Jeng, S. M., Yang, J.-M., and Aksoy, S., "Damage Mechanisms of SCS-6/Ti-6Al-4V Composites Under Thermal-Mechanical Fatigue", Materials Science and Engineering, Vol. A156, 1992, pp. 117-124.

[9] Johnson, W. S., Lubowinski, S. J., and Highsmith, A. L., "Mechanical Characterization of Unnotched SCS-6/Ti-15-3 Metal Matrix Composites at Room Temperature," Thermal and Mechanical Behavior of Ceramic and Metal Matrix Composites, ASTM STP 1080, J. M. Kennedy, H. M. Moeller, and W. S. Johnson, Eds., Philadelphia, PA, 1990.

[10] Gayda, J. and Gabb, T. P., "Isothermal Fatigue Behaviour of a $[90°]_8$ SiC/Ti-15-3 Composite at 426°C", International Journal of Fatigue, Vol. 14, Jan. 1992,, pp. 14-20.

[11] Castelli, M. G., "Thermomechanical and Isothermal Fatigue Behavior of a $[90]_8$ Titanium Matrix Composite," Proceedings of the Amercan Society for Composites, Technomic Publishing, Lancaster, PA, 1993, pp. 884-892.

[12] Schubbe, J. J. and Mall, S., "Damage Mechanisms in a Cross-Ply

Metal Matrix Composite Under Thermal-Mechanical Cycling'" Composites: Proceedings of the 8th International Conference on Composite Materials (ICCM/8), Society for the Advancement of Material and Process Engineering, Covina, CA, 1991, pp. 20-B-1 to 20-B-9.

[13] Castelli, M. G. and Ellis, J. R., "Isothermal Thermomechanical Fatigue Damage/Failure Mechanisms in SCS-6/TIMETAL 21S $[0/90]_s$ Composite," Titanium Metal Matrix Composites II, Workshop Proceedings, WL-TR-93-4105, P. R. Smith and W. C. Revelos, Eds., Wright Laboratory, Wright-Patterson Air Force Base, OH, 1993, pp. 442-456.

[14] Gayda, J., Gabb, T. P., and Lerch, B. A., "Fatigue Environment Interactions in a SiC/Ti-15-3 Composite," International Journal of Fatigue, Vol. 15, Jan. 1993, pp. 41-45.

[15] Bartolotta, P. A. and Verrilli, M. J., "Thermomechanical Fatigue Behavior of SiC/Ti-24Al-11Nb," NASA Report TM-105723, National Aeronautics and Space Administration, Lewis Research Center, Cleveland, OH, 1992.

[16] Khobaib, M. and Vahldiek, F. W., "High Temperature Oxidation Behavior of Ti_3Al Alloys," Space Age Metal Technology, Proceedings of 2nd International SAMPE Metals Conference, Society for the Advancement of Material and Process Engineering, Covina, CA, 1988, pp. 262-270.

[17] Nicholas, T. and Russ, S. M., "Elevated Temperature Fatigue Behavior of SCS-6/Ti-24Al-11Nb," Proceedings of International Conference on High-Temperature Aluminides and Intermetallics, San Diego, CA, 1991.

[18] Gabb, T. P. and Gayda, J., "Nonisothermal Fatigue Damage of SiC/Ti_3Al+Nb," NASA Report CP-10104, National Aeronautics and Space Administration, Lewis Research Center, Cleveland, OH, 1992, pp. 48-1 to 48-12.

[19] Neu, R. W. and Nicholas, T., "Thermomechanical Fatigue of SCS-6/TIMETAL 21S Under Out-of-Phase Loading," Proceedings of Symposium on Thermomechanical Behavior of Advanced Structural Materials, ASME Winter Annual Meeting, ASME, 1993.

[20] Niemann, J. T., Bowden, D. M., and Thies, D. J., "NASP Materials and Structures Augmentation Program Final Report, Titanium Matrix Composites, Vol. II-Materials and Process Development," NASP Report CR-1145, Vol. II, National Aeronautics and Space Administration, Langley Research Center, Hampton, VA, 1993.

[21] Brindley, W. J. and Smialek, J. L., "Environmental Effects on Orthorhombic Ti-22Al-23Nb," NASA Report CP-19117, National Aeronautics and Space Administration, Lewis Research Center, Cleveland, OH, 1993, pp. 34-1 to 34-12.

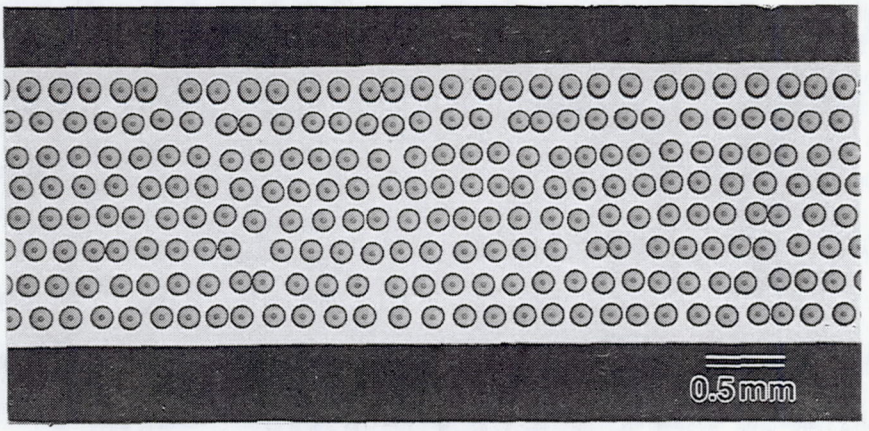

FIG. 1--SCS-6/Ti-24Al-11Nb(at.%) $[0]_8$ composite cross section.

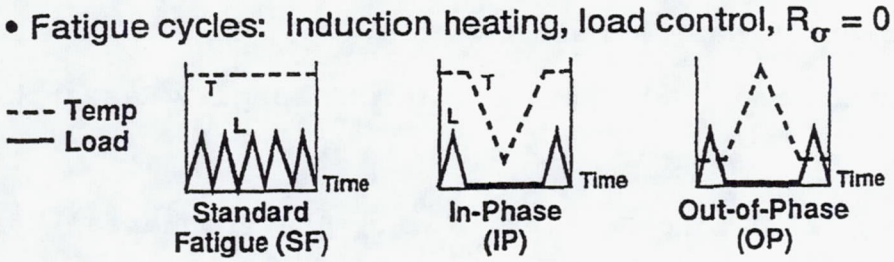

FIG. 2--Initial isothermal and nonisothermal fatigue test cycles.

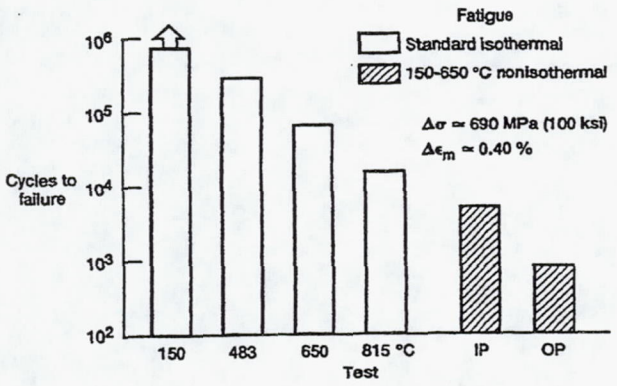

FIG. 3--Comparison of fatigue life at an approximate stress range $\Delta\sigma$ of 690 MPa and mechanical strain range $\Delta\epsilon$ of 0.40%.

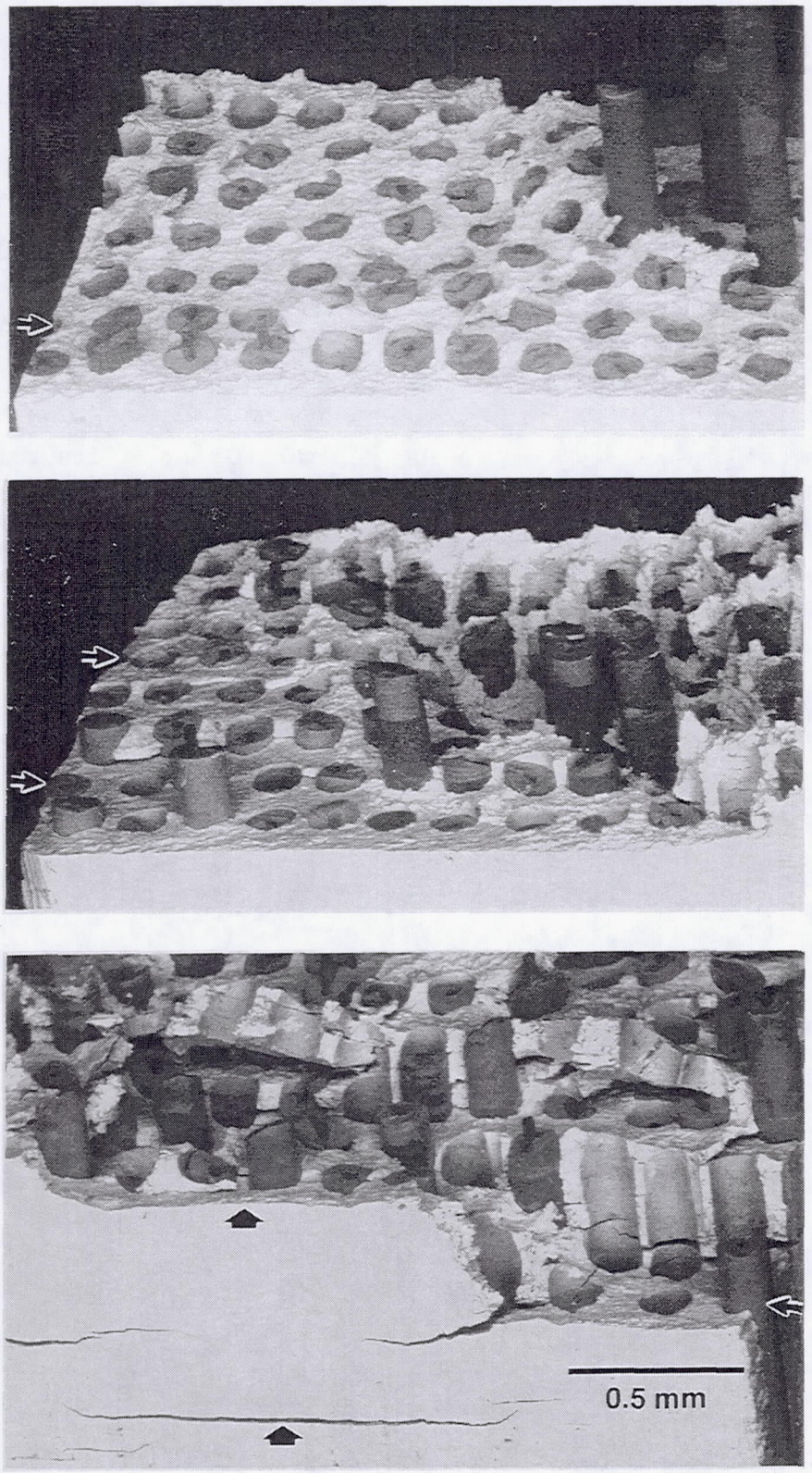

FIG. 4--Fracture surfaces of specimens tested in: a) 150°C standard isothermal fatigue, b) 650°C standard isothermal fatigue, and c) 150-650°C out-of-phase nonisothermal fatigue. Load oriented vertically.

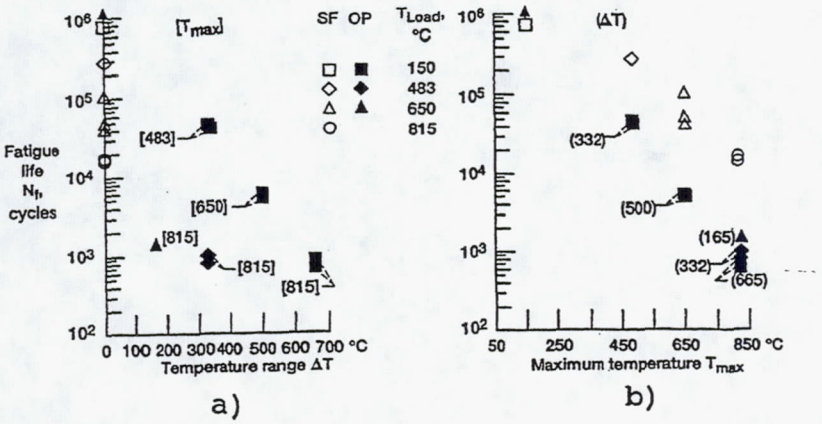

FIG. 5--Fatigue life at $\Delta\sigma \approx 690$ MPa, $\Delta\varepsilon \approx 0.40\%$ as a function of: a) temperature range ΔT, b) maximum temperature T_{max}.

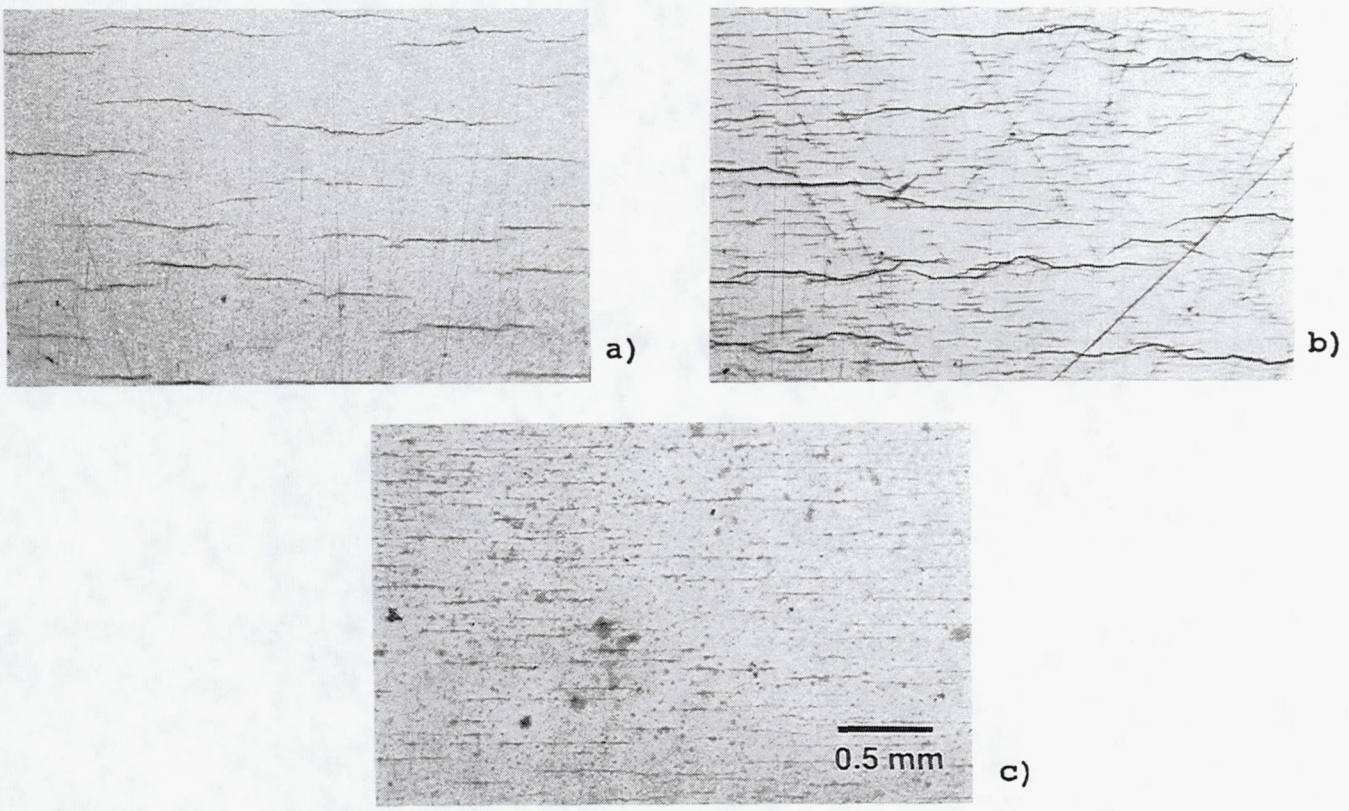

FIG. 6--Specimen gage sides after: a) 150-483°C out-of-phase nonisothermal fatigue, b) 150-815°C out-of-phase nonisothermal fatigue, c) 815°C standard isothermal fatigue. Load oriented vertically.

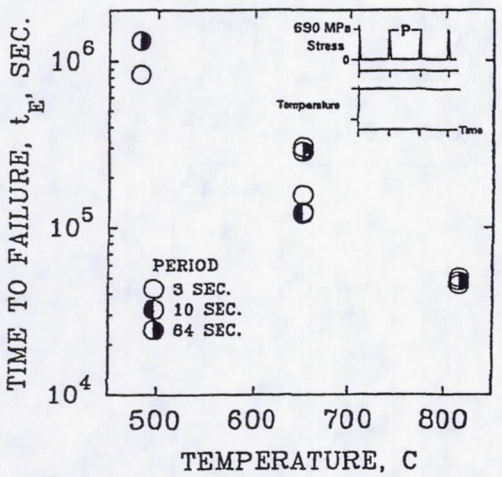

FIG. 7--Accumulated time to failure as a function of temperature in isothermal 0 load dwell tests at σ_{max}=690 MPa.

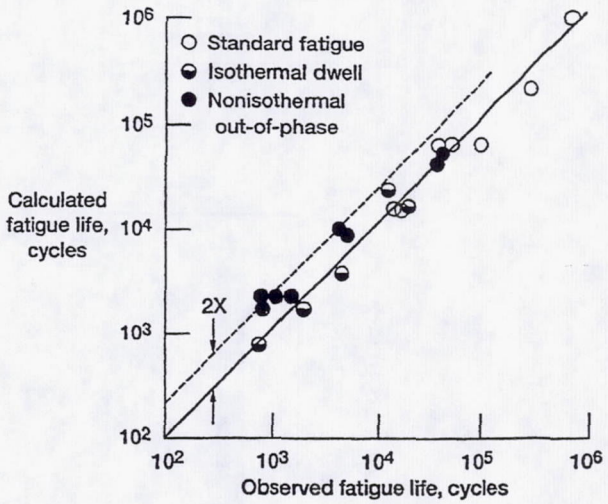

FIG. 9--Observed fatigue lives versus calculated lives.

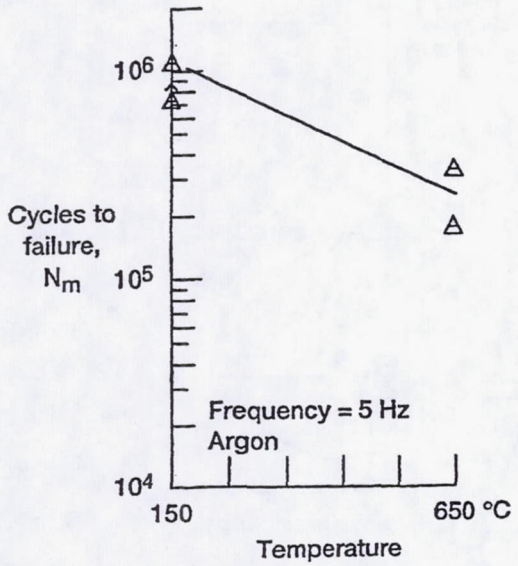

FIG. 8--Mechanical cycling life in isothermal 5 Hz tests at σ_{max}=690 MPa in argon as a function of temperature.

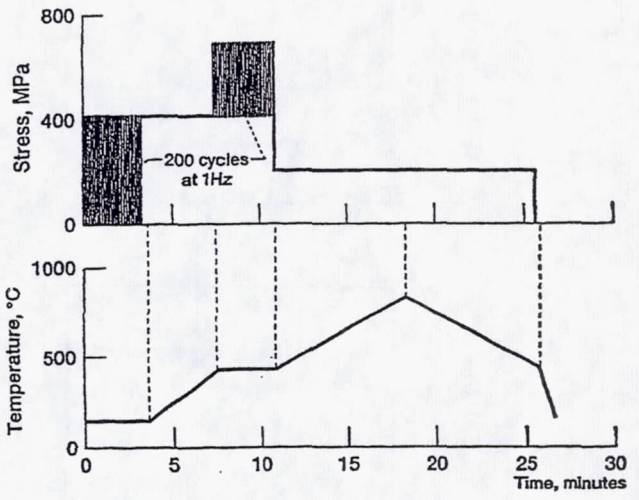

FIG. 10-- Modified ascent mission cycle [20].

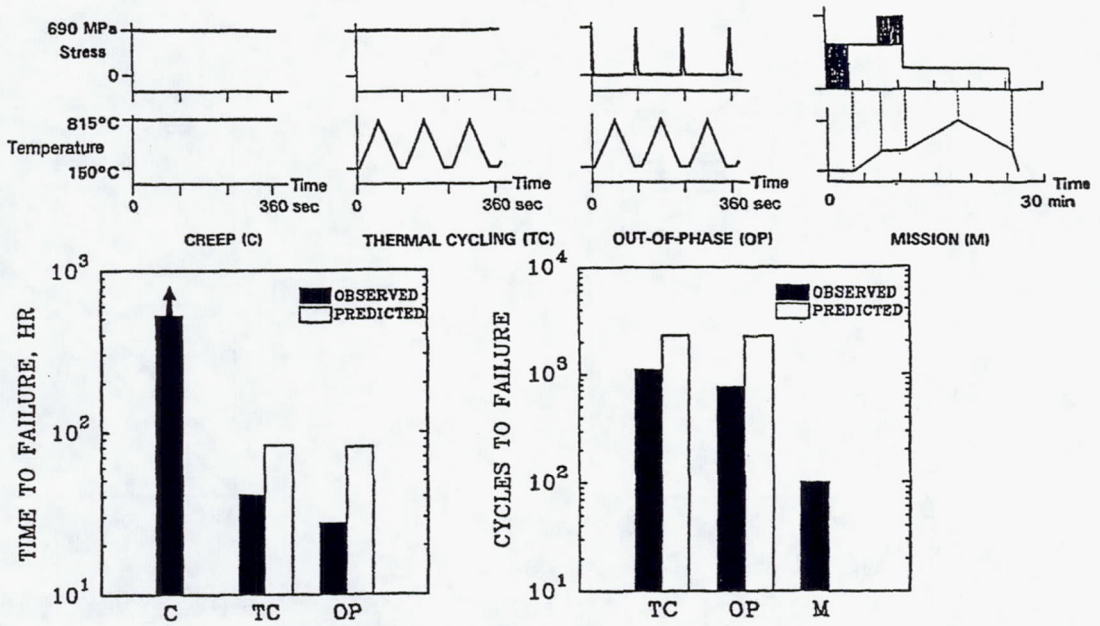

FIG. 11--Sustained load effects on life.

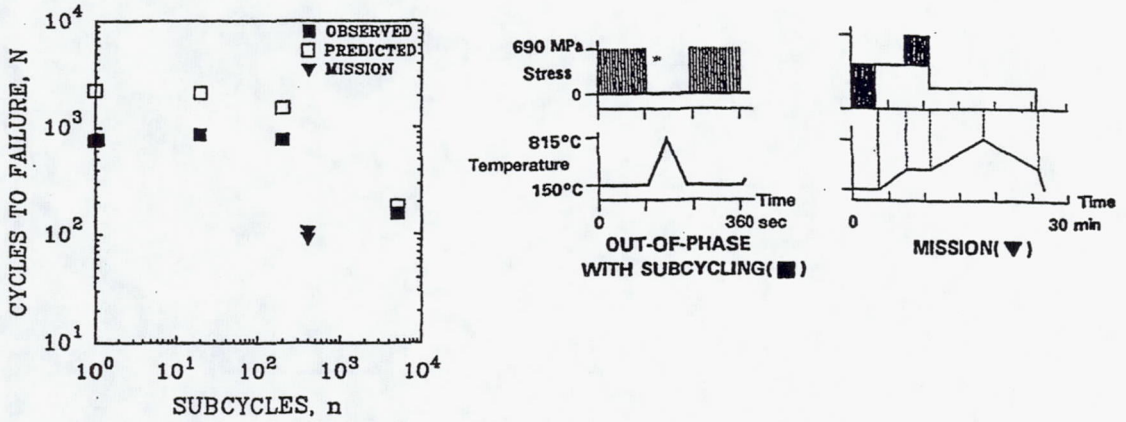

FIG. 12--Effects of subcycling on out- of-phase cyclic life(■).

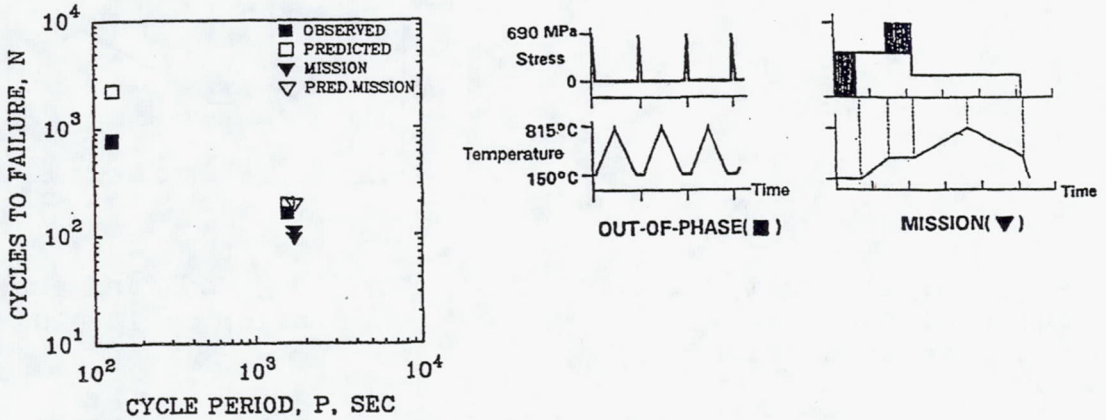

FIG. 13--Life as a function of cycle period in OP(■) and mission(▼) tests.

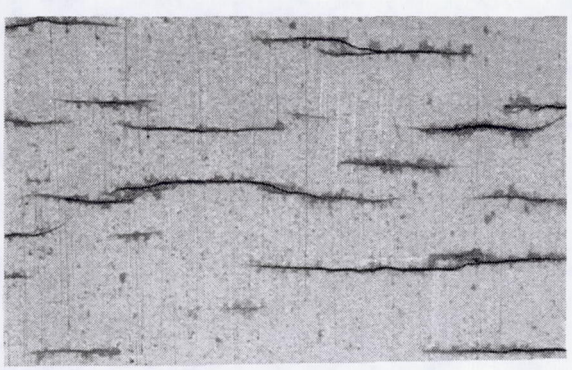

a)

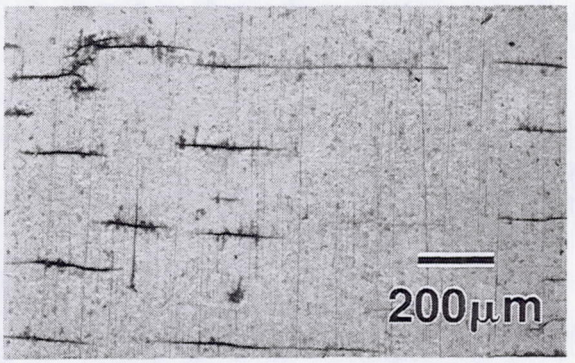

b)

FIG. 14--Gage sides after fatigue tests with σ_{max} ≈690 MPa, 26 minute cycle period: a) OP, b) mission.

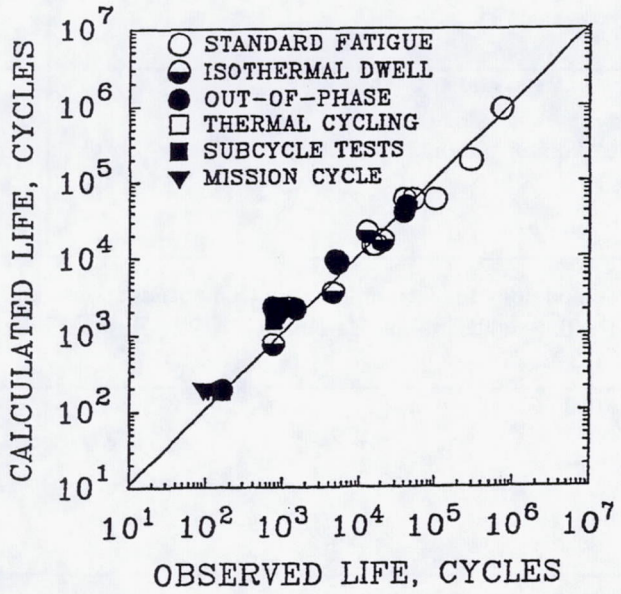

FIG. 15--Observed fatigue lives versus calculated lives.

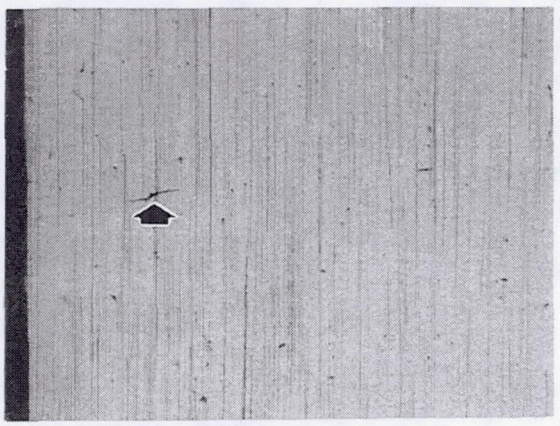

a)

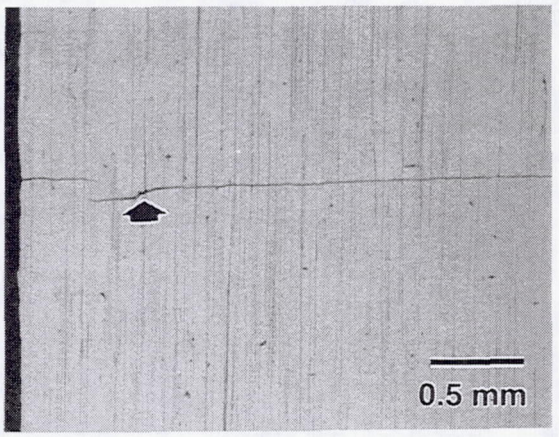

b)

FIG. 16--Gage surfaces after: a) 750 thermal cycles at 0 load from 150-815°C, b) above plus 739,000 fatigue cycles, 150°C, $\Delta\sigma$=690MPa.

REPORT DOCUMENTATION PAGE

Form Approved
OMB No. 0704-0188

1. AGENCY USE ONLY (*Leave blank*)	2. REPORT DATE	3. REPORT TYPE AND DATES COVERED
	February 1994	Technical Memorandum

4. TITLE AND SUBTITLE

Matrix Fatigue Cracking Mechanisms of α_2 TMC for Hypersonic Applications

5. FUNDING NUMBERS

WU–505–63–1A

6. AUTHOR(S)

Timothy P. Gabb and John Gayda

7. PERFORMING ORGANIZATION NAME(S) AND ADDRESS(ES)

National Aeronautics and Space Administration
Lewis Research Center
Cleveland, Ohio 44135–3191

8. PERFORMING ORGANIZATION REPORT NUMBER

E–8610

9. SPONSORING/MONITORING AGENCY NAME(S) AND ADDRESS(ES)

National Aeronautics and Space Administration
Washington, D.C. 20546–0001

10. SPONSORING/MONITORING AGENCY REPORT NUMBER

NASA TM–106506

11. SUPPLEMENTARY NOTES

Prepared for Life Prediction Methodology for Titanium Matrix Composites sponsored by the American Society for Testing and Materials, Hilton Head, South Carolina, March 22–24, 1994. Responsible person, Timothy P. Gabb, organization code 5120, (216) 433–3272.

12a. DISTRIBUTION/AVAILABILITY STATEMENT

Unclassified - Unlimited
Subject Categories 24 and 26

12b. DISTRIBUTION CODE

13. ABSTRACT ***(Maximum 200 words)***

The objective of this work was to understand matrix cracking mechanisms in a unidirectional α_2 TMC in possible hypersonic applications. A $[0]_8$ SCS-6/Ti-24Al-11Nb(at.%) TMC was first subjected to a variety of simple isothermal and nonisothermal fatigue cycles to evaluate the damage mechanisms in simple conditions. A modified ascent mission cycle test was then performed to evaluate the combined effects of loading modes. This cycle mixes mechanical cycling at 150 and 483 °C, sustained loads, and a slow thermal cycle to 815 °C. At low cyclic stresses and strains more common in hypersonic applications, environment-assisted surface cracking limited fatigue resistance. This damage mechanism was most acute for out-of-phase nonisothermal cycles having extended cycle periods and the ascent mission cycle. A simple linear fraction damage model was employed to help understand this damage mechanism. Time-dependent environmental damage was found to strongly influence out-of-phase and mission life, with mechanical cycling damage due to the combination of external loading and CTE mismatch stresses playing a smaller role. The mechanical cycling and sustained loads in the mission cycle also had a smaller role.

14. SUBJECT TERMS

Fatigue, Thermomechanical; Composite; Hypersonic

15. NUMBER OF PAGES

29

16. PRICE CODE

A03

17. SECURITY CLASSIFICATION OF REPORT	18. SECURITY CLASSIFICATION OF THIS PAGE	19. SECURITY CLASSIFICATION OF ABSTRACT	20. LIMITATION OF ABSTRACT
Unclassified	Unclassified	Unclassified	